

MAXIMUM SPEED OF BATTERY-POWERED TILT-ROTOR AIRCRAFT

Nahyeon Roh¹, Minjun Park²

^{1,2} Hanwha Systems Co., Ltd.

Abstract

The closed form maximum flight speed formulae have been derived for use in the conceptual design phase. The formulas have been derived to calculate the maximum flight speed that satisfies both the available power and torque of the designed aircraft. To this end, assumptions are proposed to simplify the formula and the suitability of the proposed assumptions is verified. It is assumed that the nacelle is aligned with the freestream direction and that the propeller advance ratio and efficiency are constant. An analysis of the maximum flight speed variation due to available power and torque is presented for demonstration. The effect of the advance ratio is also assessed. The demonstration confirms that the maximum flight speed is determined by the available power or torque constraints. The higher advance ratio requires higher torque for a given available power. With sufficient available power, the higher advance ratio results in a slower maximum flight speed for a given available torque.

Keywords: aircraft design, maximum flight speed, tilt-rotor

1. Introduction

The increasing demand driven by advancements in battery technology and the need to address urban traffic congestion has increased interest in electric vertical takeoff and landing (eVTOL) aircraft. In line with this trend, various concepts of eVTOLs with different operational concepts and powertrain architectures, distinct from traditional fixed-wing or rotorcraft, are being proposed. Unlike traditional rotorcrafts that combine a gas turbine engine and a large rotor, the distributed propulsion with multiple rotors, propellers, or fans combined with a motor is mainly considered the propulsion system for urban air mobility (UAM). The electric distributed propulsion system is advantageous for noise reduction and safety [1-3]. Furthermore, the application of motors increases the freedom in controlling the rotating speed of the propeller. Unlike traditional aircraft, which can only operate at a rotating speed set by a designed gearbox, motors can control the rotating speed through the input of current and voltage [4]. In other words, the application of motors offers advantages, such as the ability to adjust rotating speeds based on flight speed for optimal efficiency in operation [5, 6]. These configurations can be categorized into tilt-rotors with tilting propellers to obtain both lift and thrust, lift-cruise which feature separate propellers for lift and thrust, and multi-rotor types that utilize propellers solely for generating lift [7]. In particular, the tilt-rotor type, which tilts the propellers based on the flight mode, does not require additional propellers for lift and thrust. This design allows for weight reduction and eliminates drag caused by stopped propellers for lift, resulting in a higher cruise speed compared to other designs [8].

It is necessary to design configurations that meet requirements and evaluate numerous parameters. Therefore, rapid conceptual design tools are essential. Various simplified design exploration methods for distributed electric propulsion [9] and sizing techniques [10-14] have been developed for utilization in the conceptual design phase. These tools determine the total power, torque, and energy required for each configuration to meet the specified requirements. Once the design is complete, validation is required to assess the maximum distance, endurance, and speed. Formulas for the maximum performance of traditional aircraft are well-established [15-18]. However, obtaining the maximum performance for a new type of aircraft with distributed propulsion based on batteries

MAXIMUM SPEED OF BATTERY-POWERED TILT-ROTOR

and motors requires some modifications to existing formulas. Numerous studies have been conducted on the maximum flight distance and maximum endurance [19-28]. The maximum flight speed is suggested as a result of parameter studies along with battery specific energy [29] or MTOW [30]. However, research has been absent in formulating equations for the maximum flight speed of eVTOL aircraft.

This study aims to derive the formula for the maximum flight speed of a tilt-rotor type electric-powered aircraft with determined available power and torque. Assumptions and simplified equilibrium equations are applied to reduce the complexity of deriving formulas. Parameter studies are then carried out to demonstrate the potential application of the derived formulas.

2. Configuration and flight condition

The analysis is based on a designed electric powered quad tilt-rotor with a predetermined configuration, normal cruise speed, and required power and torque. The specifications are summarized in Table 1. In this paper, "propeller" is used instead of "tilt-rotor" since the discussions in this paper mainly focus on the cruise conditions. Under the normal cruise condition, the freestream velocity is assumed parallel to the natural horizon. It means that the angle of attack is the same as pitch attitude. Therefore, pitch attitude is used instead of angle of attack to emphasize the control of pitch attitude during maximum flight speed. An arbitrary propeller that could achieve more than 0.8 for both FM and propeller efficiency are designed. The chord distribution and twist distribution of a propeller are shown in Fig. 1.

3. Assumptions

3.1 Simplification of equilibrium equations

It is assumed that the nacelle tilt angle aligns with the freestream direction to take advantage of simplified equilibrium equation. In other words, even though the pitch attitude is adjusted to generate enough lift according to freestream velocity, the propellers' thrust direction is constantly parallel to the drag direction. To verify the feasibility of applied assumption, aerodynamic performance was compared.

Table 1 - Configuration information

Configurations			
MTOW [kg]	3175	Propeller radius [m]	3
Reference area [m ²]	25.2	No. motors	4
Aspect ratio	11.3	No. propellers	4
Lift slope	5.27	No. blades	5
Oswald efficiency	0.72		
Flight conditions under normal cruise condition			
Density [kg/m ³]	1.0	Pitch attitude [°]	0
Gravity acceleration [m/s ²]	9.8	Flight speed [m/s]	67
Lift-to-drag ratio	15	Advance ratio	4.12
Efficiencies			
Electric efficiency	0.85		

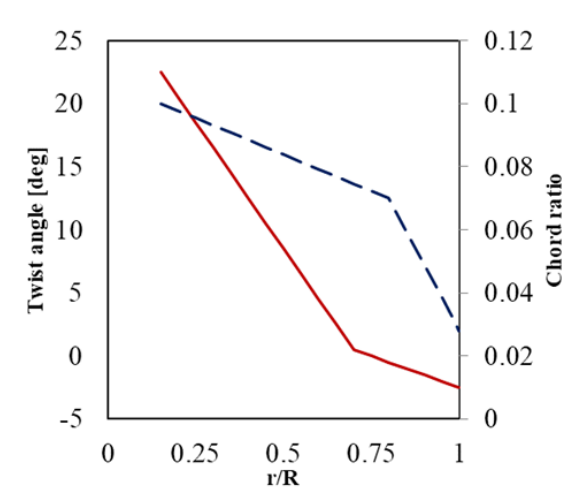


Figure 1 – Propeller radial distribution

Prior to formulating equations along with flight conditions, some aerodynamic coefficients related to viscosity are obtained based on the assumptions for normal cruise condition. Since the angle of attack has been replaced by the pitch attitude, the lift is defined as Eq. (1).

$$L = \frac{1}{2} \rho \, SV_{\infty}^2 (C_{L0} + C_{L\alpha} \theta) \tag{1}$$

Under normal cruise condition, pitch attitude is assumed to be 0° . Therefore, C_{L0} is obtained as Eq. (2) by rearranging the Eq. (1).

$$C_{L0} = mg/(\frac{1}{2}\rho \, SV_{\infty}^2) \tag{2}$$

The drag is defined as Eq. (3) by applying thin airfoil theory [32].

$$D = \frac{1}{2} \rho \, SV_{\infty}^{2} \left[C_{D0} + \frac{1}{\pi eAR} (C_{L0} + C_{L\alpha} \Theta)^{2} \right]$$
 (3)

In a similar manner to the calculation of C_{L0} , C_{D0} is obtained by restructuring Eq. (2) and inserting Eq. (3). It is expressed by Eq. (4) when $D = L/(L/D)_{cruise}$ and L = mg by equilibrium equation.

$$C_{D0} = \frac{mg}{1/2 \rho \, SV_{\infty}^2 (L/D)_{Cruise}} - \frac{C_{L0}^2}{\pi e A R} \tag{4}$$

For the actual flight condition, the equilibrium equation is defined as Eq. (5) and (6).

$$L = mg - T\sin\Theta \tag{5}$$

$$D = T\cos\Theta \tag{6}$$

By replacing the thrust in Eq. (6) with the expression represented by the drag, the equilibrium equation is consolidated into Eq. (7).

$$L = mg - D(\sin\theta / \cos\theta) \tag{7}$$

If a small pitch attitude assumption is applied, it is possible to denote as Eq. (8) by inserting Eq. (1) and (3). Note that, in this condition, the freestream velocity may not always be the same as in the normal cruise condition, as it could represent the maximum flight speed.

$$\frac{1}{2} \rho \, SV_{\infty}^{2} (C_{L0} + C_{L\alpha} \Theta) + \frac{1}{2} \rho \, SV_{\infty}^{2} \left[C_{D0} + \frac{1}{\pi e A R} (C_{L0} + C_{L\alpha} \Theta)^{2} \right] \Theta = mg \tag{8}$$

It could be rearranged for pitch attitude as Eq. (9).

$$\frac{1}{\pi eAR} C_{L_{\alpha}}^{2} \Theta^{3} + 2 \frac{1}{\pi eAR} C_{L0} \Theta^{2} + \left(C_{L_{\alpha}} + C_{D0} + \frac{1}{\pi eAR} C_{L0}^{2} \right) \Theta + C_{L0} - \frac{mg}{1/2 \rho SV_{\infty}^{2}} = 0$$
 (9)

The coefficients of each term in Eq. (9) are denoted as A, B, C, and D to obtain the exact solution for pitch attitude. The pitch attitude is acquired through Eq. (10), excluding complex or non-physical solutions.

$$\Theta = \frac{(\operatorname{sqrt}((-27 \, A^2D + 9 \, A \, B \, C - 2 \, B^3)^2 + 4 \, (3 \, A \, C - B^2)^3) - 27 \, A^2D + 9 \, A \, B \, C - 2 \, B^3)^{\frac{1}{3}}}{3 \, 2^{\frac{1}{3}}A}$$

$$- \frac{2^{\frac{1}{3}}(3 \, A \, C - B^2)}{3 \, A \, (\operatorname{sqrt}((-27 \, A^2D + 9 \, A \, B \, C - 2 \, B^3)^2 + 4 \, (3 \, A \, C - B^2)^3) - 27 \, A^2D + 9 \, A \, B \, C - 2 \, B^3)^{\frac{1}{3}}}{-\frac{B}{3 \, A}}$$

$$(10)$$

The solution for the fourth-order equation regarding pitch attitude is derived in a highly complex form. It leads to the derivation of equations of the fifth order or higher as the influence of pitch attitude cannot be separated when calculating power and torque. Since obtaining an exact solution for a fifth-order or higher equation is not feasible [33], the actual flight condition is unsuitable for deriving a maximum flight speed with a closed-form solution.

On the other hand, the equilibrium equation under the assumed flight condition is suggested in a more straightforward form as D=T and L=W. Therefore, the pitch attitude is derived as Eq. (11) by rearranging $C_L = C_{L0} + C_{L\alpha}\theta$, when $C_L = mg/(1/2 \rho SV_{\infty}^2)$.

$$\Theta = \frac{C_L - C_{L0}}{C_{L\alpha}} \tag{11}$$

Drag is calculated using Eq. (12). This is possible since the lift coefficient is derived from $C_L = mg/(1/2 \, \rho \, SV_\infty^2)$, without considering the pitch attitude.

$$D = \frac{1}{2} \rho \, SV_{\infty}^2 \left[C_{D0} + \frac{1}{\pi e A R} \, C_L^2 \right] \tag{12}$$

Figure 2 compares the predicted pitch attitude and power obtained through both flight conditions. To assess the influence of flight speed reflecting nacelle angle control, limits imposed by available power and torque are neglected. Through the figure, it can be seen that the pitch attitude at cruising speed is 0° according to the applied assumption. As the flight speed increases, the pitch attitude gradually

MAXIMUM SPEED OF BATTERY-POWERED TILT-ROTOR

decreases due to the increase in dynamic pressure. The required power gradually increases with the increase in both flight speed and required thrust. This indicates that the derived formulas well reflect the general trend for flight speed. The difference in pitch attitude is less than 3.4%, and the difference in required power is less than 0.6% across the analyzed range. Therefore, the assumed flight condition, which permits a simplified formula, is applied for further study as the difference is negligible.

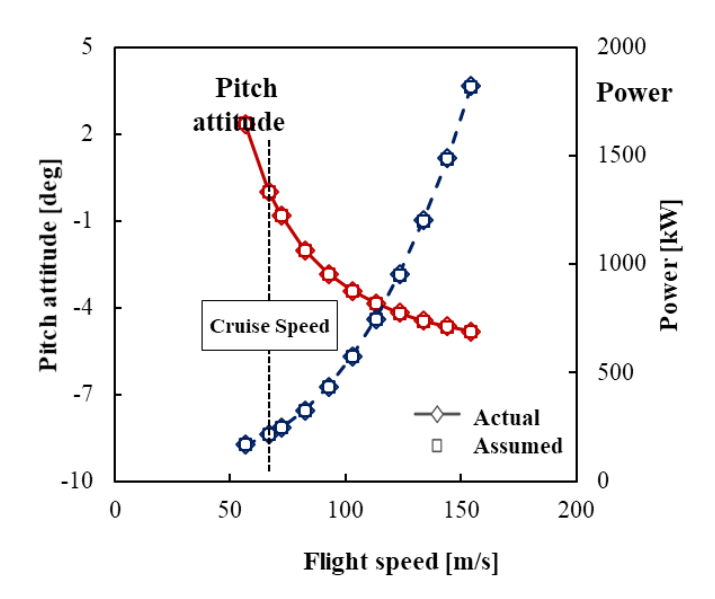


Figure – 2 Pitch attitude and power in accordance with flight speed

3.2 Applying constant advance ratio

In order to minimize the change in propeller efficiency at maximum flight speed, the advance ratio is assumed to be constant under all flight conditions. The propeller efficiency of conventional aircraft decreases with increasing flight speed. However, if advance ratio is constant and the thrust is proportional to the square of the freestream speed, the propeller efficiency is constant.

The total drag is expressed as the sum of the parasite drag and the induced drag which proportional and inversely proportional to the square of the freestream velocity, respectively. As the maximum flight speed is determined by the speed at minimum drag, the maximum flight speed is the speed thereafter. This means that the drag near the maximum flight speed is dominated by the parasite drag. Since it is assumed that T=D and the drag is defined by Eq. (12), it can be assumed that the thrust near the maximum flight speed is proportional to the square of the freestream velocity. Therefore, the assumption of a constant advance ratio can be suggested as a way to minimize the change of propeller efficiency.

Figure 3 presents a comparison of propeller efficiency under the constant rotating speed and constant advance ratio. The rotating speed and advance ratio are selected based on the normal cruise conditions of the design aircraft. For a constant rotating speed, 160 RPM is considered for all analysis conditions, with the advance ratio increasing from 3.5 to 9.7. When a constant advance ratio of 4.21 is considered, the rotating speed increases from 130 RPM to 360 RPM.

The figure illustrates that the change in efficiency is relatively minor when the advance ratio remains constant. At the maximum flight speed to normal cruise conditions when rotating at a constant speed, the efficiency decreases by 31%, while at a constant advance ratio, the efficiency decreases by 6.1%. Furthermore, the change in propeller efficiency after the cruise speed is evident. This is due to the fact that the target thrust is more proportional to the square of the freestream velocity.

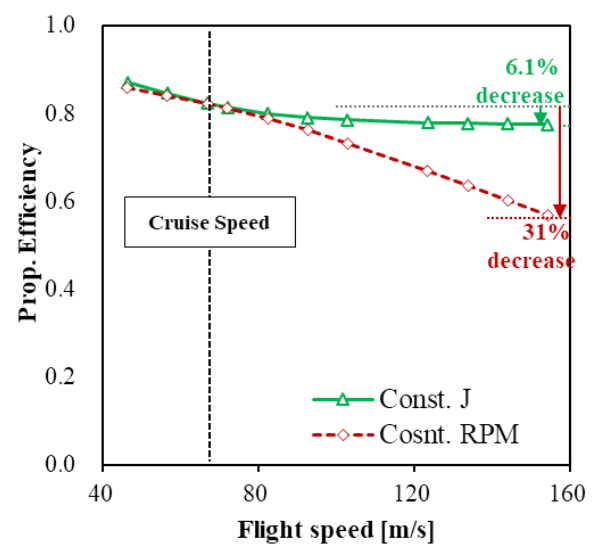


Figure – 3 Comparison of propeller efficiency

4. Derivation of maximum flight speed equation

In the case of performing a table-lookup on propeller efficiency, iterative calculation for propeller efficiency convergence is required to calculate the maximum flight speed using the available power and torque. On the other hand, if efficiency is assumed to be constant, exact solutions can be obtained that do not require repeated calculations. The previous chapter shows that the variation of propeller efficiency with flight speed is negligible for a constant advance ratio. In order to derive a simple formula for application in the conceptual design phase, the formulas assuming constant propeller efficiency are derived.

The maximum flight speed is defined as the speed at which the aircraft is capable of flying with the maximum power or maximum torque. This implies that the required power or torque for the maximum flight speed match the available power or torque. Furthermore, both the required power and torque should be less than the available power and torque. While the velocity satisfies the maximum power constraints, the corresponding torque determined could be greater than the available torque. Conversely, if the velocity indicates an aircraft in flight with maximum torque, the required power could exceed the available power. Consequently, the maximum flight speed that satisfies both available power and torque requirements is determined by selecting the lower of the two velocities as Eq. (13).

$$V_{max} = \min(V_{max, power}, V_{max, torque})$$
 (13)

The torque and power for each condition, whether utilizing maximum power or maximum torque, are calculated by considering the rotating speed that ensures the same advance ratio as in normal cruise condition. In other words, the rotating speeds of each condition are different. Maximum flight speeds satisfying the available power and torque are derived separately to calculate speed that satisfies both conditions.

4.1 Maximum flight speed with available power

Inserting Eq. (12) into the power equation results in Eq. (14), where P = TV and D = T.

$$P_{req} = \frac{D V_{max}}{\eta_{all}} = \frac{1}{\eta_{all}} \left[C_{D0} \left(\frac{1}{2} \rho V_{max}^2 S \right) + \frac{1}{\pi e A R} \frac{(mg)^2}{\frac{1}{2} \rho V_{max}^2 S} \right] V_{max}$$
 (14)

The $V_{\rm max}$ is the maximum velocity that satisfies maximum power or maximum torque. The η_{all} is the cross of propeller and electric efficiency. The required power from Eq. (14) is substituted with the determined available power to derive a closed-form solution to calculate the maximum velocity the

available power allows. Rearranging in terms of maximum flight speed yields the expression given by Eq. (15).

$$V_{max,power}^{4} - \frac{2\eta_{all}P_{avail}}{C_{D0}\rho S}V_{max,power} + \frac{1}{\pi eAR} \frac{4(mg)^{2}}{C_{D0}\rho^{2}S^{2}} = 0$$
 (15)

Consequently, the maximum velocity that available power allows is obtained by solving Eq. (15).

4.2 Maximum flight speed with available torque

The propeller angular speed is defined as Eq. (16), assuming the same advance ratio is used in normal cruise condition.

$$\Omega = \frac{V_{\text{tip}}}{R} = \frac{1}{R} \frac{V_{\infty}}{I} \pi \tag{16}$$

The power is expressed as Eq. (17) by inserting Eq. (16) to reflect the available torque of each motor.

$$P_{req} = Q_{avail} N_{motor} \Omega = Q_{avail} N_{motor} \frac{1}{R} \frac{V_{\infty}}{J} \pi$$
 (17)

Inserting Eq. (17) into Eq. (14) results in Eq. (18).

$$Q_{avail} N_{motor} \frac{1}{R} \frac{V_{\infty}}{J} \pi = \frac{1}{\eta_{all}} \left[C_{D0} \left(\frac{1}{2} \rho V_{\infty}^2 S \right) + \frac{1}{\pi e A R} \frac{(mg)^2}{\frac{1}{2} \rho V_{\infty}^2 S} \right] V_{\infty}$$
 (18)

Rearranging Eq. (18) to maximum speed yields Eq. (19).

$$\frac{1}{4}\rho^{2}S^{2}C_{D0}V_{max,torque}^{4} - Q_{avail}N_{motor}\frac{1}{R}\frac{1}{I}\pi\eta_{all}\frac{1}{2}\rho SV_{max,torque}^{2} + \frac{1}{\pi eAR}(mg)^{2} = 0 \quad (19)$$

The closed form equation for the maximum velocity that the available torque allows is obtained by solving Eq. (19), which is the 4th order equation for $V_{\text{max,torque}}$.

4.3 Comparison of maximum speed

The maximum flight speed obtained by performing a table-lookup on the propeller efficiency and the assuming the constant efficiency are compared. Fig. 4 illustrates the maximum flight speeds as a function of available power and torque. Through the figure, it can be seen that the differences between the two method are insignificant. For the maximum speed constraint by available power and torque, the average error by applying a constant advance ratio is 0.8% and 1.5%, respectively. From the comparison, it is concluded that the applied assumption is reliable in qualitatively and quantitatively.

5. Demonstration

The demonstration is conducted to present the usefulness of derived formulas. The analysis ranges for power and torque are selected to refer to the conceptual design of UAM [34-36]. All values, aside

from the pitch attitude and lift-to-drag ratios that differ with flight speed, are applied with the same as presented in Table 1.

The maximum speed in accordance with torque is illustrated in Fig. 5. The impact of the advance ratio and the maximum speed due to available power are also compared. For a designed aircraft, different values of the advance ratio imply variations in the propeller efficiency. However, in this demonstration, all input values are kept the same except for the advance ratio to present its impact solely on the formula. The maximum flight speed limited by available torque is represented by solid lines with markers, while that determined by available power is depicted by dashed lines. The result shows that the maximum speed determined by power remains constant for all torques, as it is not affected by the advance ratio and available torque. Assuming an aircraft with an advance ratio of 4.2 and available power of 1200 kW, the maximum flight speed increases with the increase in torque until it reaches 9000 Nm. However, when the torque exceeds 9000 Nm, the maximum flight speed is limited to 140 m/s since the speed determined by available power becomes smaller. All available torque is utilized up to 9000 Nm, and beyond this point, there is a margin in torque as the required torque has a relatively minor value compared to the available torque. The intersection point of the solid and dashed lines represents the point at which both available power and torque are fully utilized to achieve the maximum flight speed. For the comparison of the influence of the advance ratio, three different advance ratios are compared. It can be seen that a larger torque is required to achieve the same maximum speed with a higher advance ratio for the same available power. In cases where the available torque is the same, a higher advance ratio results in a slower maximum flight speed under

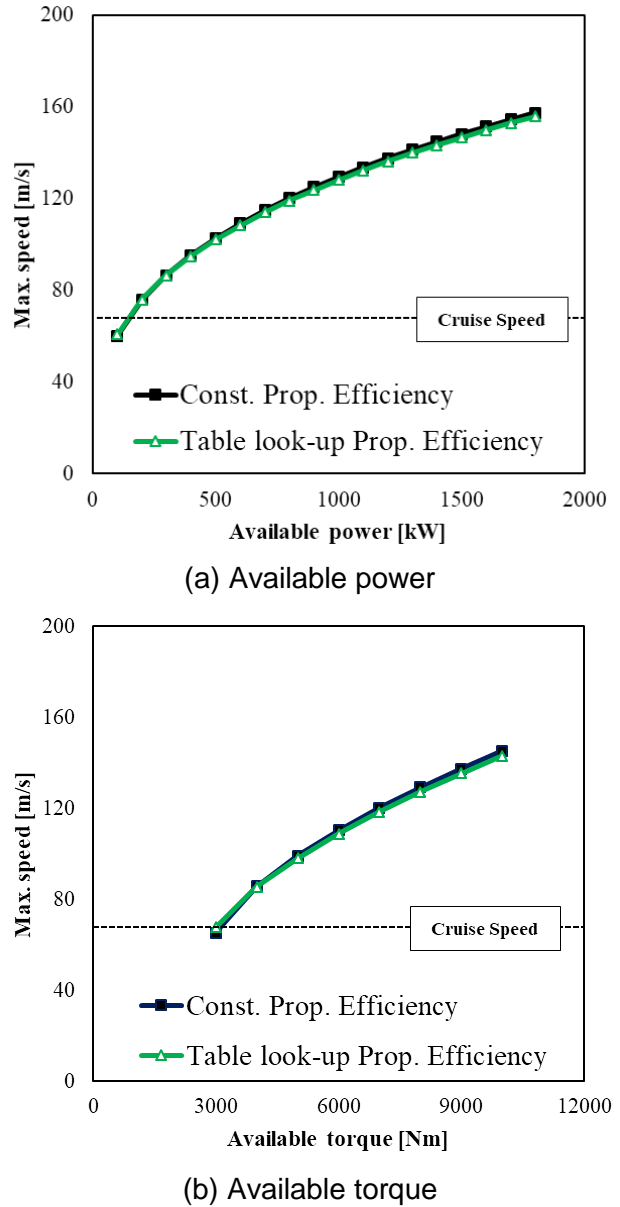


Figure – 4 Comparison of maximum flight speed

conditions that the available power has enough margin. It is based on the relationship between advance ratio and torque, which can be derived through Eq. (22).

Through demonstrations, it is confirmed that the derived equations show trends that satisfy the fundamental theorem. The analysis presented in this manner is expected to help predict the maximum flight speed for the designed aircraft.

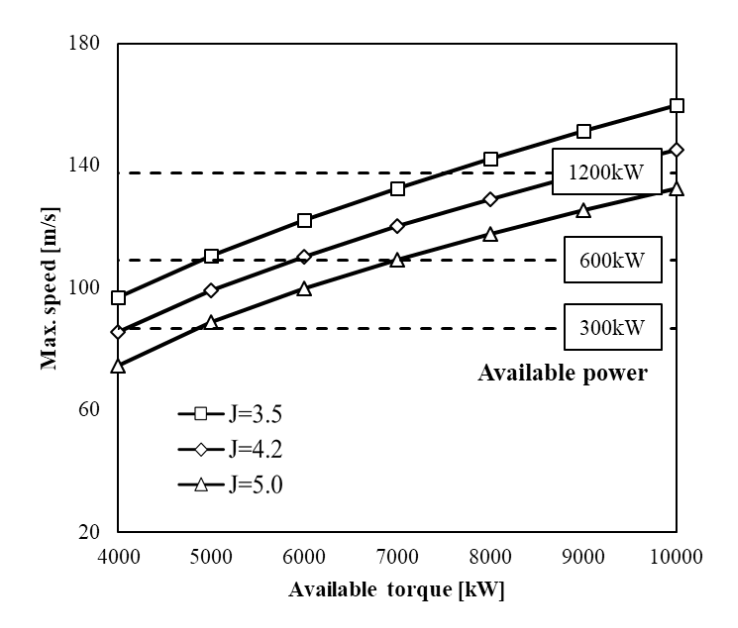


Figure 5 – Variation of maximum flight speed with various advance ratios

6. Conclusion

The objective of this study was to derive closed-form formulas for maximum flight speed, with the intention of applying them during the conceptual design phase. To this end, assumptions were presented for simplifying the formulas and their suitability was verified. The nacelle tilt angle was assumed to align with the freestream direction, which allows for the simplification of pitch attitude calculations and the derivation of a closed-form solution for maximum flight speed. The discrepancy between the proposed assumption and the actual flight condition in terms of airframe pitch attitude was less than 3.4%, and less than 0.6% in required power. A constant advance ratio and propeller efficiency were assumed. The difference in maximum flight speed between performing a table-lookup on the propeller efficiency and assuming a constant efficiency was less than 1.5%.

The formulas have been derived to calculate the maximum flight speed that satisfies both available power and torque of the designed aircraft. An analysis of the maximum flight speed variation due to available power and torque was presented for demonstration. The effect of the advance ratio was also assessed. The demonstration confirmed that maximum flight speed is determined by available power or torque constraints. The higher advance ratio requires a higher torque for a given available power. With sufficient available power, the higher advance ratio leads to a slower maximum flight speed for a given available torque.

This study is limited in that it does not account for efficiency changes due to 3D effects from the propeller, thereby neglecting variations in propeller efficiency at the same advance ratio. Nevertheless, the results provide insight into the maximum flight speed of a designed aircraft during the conceptual design phase. While the demonstration is specific to the generic quad tiltrotor eVTOL aircraft, the derived formulas are applicable universally to various eVTOL aircraft. It would be suitable for rapid prediction of maximum flight speed.

7. Funding Sources

This research was conducted with the support of the Ministry of Land, Infrastructure and Transport/Korea Agency for Infrastructure Technology Advancement (Project Number: RS-2022-00143965).

References

- [1] Gohardani, A. S., Georgios D., and Riti S., "Challenges of future aircraft propulsion: A review of distributed propulsion technology and its potential application for the all electric commercial aircraft." Progress in Aerospace Sciences, Vol 47, No. 5, 2011, pp. 369-391.
- [2] Brelje, B. J., & Martins, J. R., "Electric, hybrid, and turboelectric fixed-wing aircraft: A review of concepts, models, and design approaches," Progress in Aerospace Sciences, Vol. 104, 2019, pp. 1-19.
- [3] Vieira, D. R., Silva, D., & Bravo, A., "Electric VTOL aircraft: the future of urban air mobility (background, advantages and challenges)," International Journal of Sustainable Aviation, Vol. 5, No. 2, 2019, pp. 101-118.
- [4] Kim, H. D., Perry, A. T., & Ansell, P. J. "A review of distributed electric propulsion concepts for air vehicle technology," In 2018 AIAA/IEEE Electric Aircraft Technologies Symposium (EATS), IEEE, Cincinnati, OH, 2018, pp. 1-21.
- [5] Stepniewski, W. Z., and C. N. Keys. Rotary-wing aerodynamics, Courier Corporation, 1984.
- [6] Rendón, M. A., Sánchez R, C. D., Gallo M, J., & Anzai, A. H., "Aircraft hybrid-electric propulsion: Development trends, challenges and opportunities," Journal of Control, Automation and Electrical Systems, Vol. 32, No. 5, 2021, pp. 1244-1268.
- [7] Johnson, W., & Silva, C., "NASA concept vehicles and the engineering of advanced air mobility aircraft," The Aeronautical Journal, Vol. 126, No. 1295, 2022, pp. 59-91.
- [8] Bao, W., Wang, W., Chen, X., Zhang, H., & Zhao, Q., "Numerical analyses of aeroacoustic characteristics of tiltrotor considering the aerodynamic interaction by the fuselage in hover," Aerospace Science and Technology, Vol. 141, 2023.
- [9] Isikveren, A. T., "Method of Quadrant-Based Algorithmic Nomographs for Hybrid/Electric Aircraft Predesign," Journal of Aircraft, Vol. 55, No. 1, 2018, pp. 396–405.
- [10] Silva, C., & Johnson, W., "Practical Conceptual Design of Quieter Urban VTOL Aircraft," In Vertical Flight Society's 77th Annual Forum & Technology Display, Online, 2021
- [11] Bryson, D. E., Marks, C. R., Miller, R. M., and Rumpfkeil, M. P., "Multidisciplinary Design Optimization of Quiet, Hybrid Electric Small Unmanned Aerial Systems," Journal of Aircraft, Vol. 53, No. 6, 2016, pp. 1959–1963.
- [12] Palaia, G., Abu Salem, K., Cipolla, V., Binante, V., & Zanetti, D., "A conceptual design methodology for e-VTOL aircraft for urban air mobility," Applied Sciences, Vol. 11, No. 22, 2021, pp. 10815.
- [13] de Vries, R., Brown, M., and Vos, R., "Preliminary Sizing Method for Hybrid-Electric Distributed-Propulsion Aircraft," Journal of Aircraft, Vol. 56, No. 6, 2019, pp. 2172–2188.
- [14] Finger, D. F., Braun, C., and Bil, C., "An Initial Sizing Methodology for Hybrid-Electric Light Aircraft," 2018 Aviation Technology, Integration, and Operations Conference, AIAA Paper 2018-4229, June 2018.
- [15] Roskam, J., Airplane Design: Part 6-Preliminary Calculation of Aerodynamic, Thrust and Power Characteristics, DAR corporation, 1985
- [16] Raymer, D., Aircraft design: a conceptual approach, American Institute of Aeronautics and Astronautics, Inc.
- [17] Torenbeek, E., Synthesis of subsonic airplane design: an introduction to the preliminary design of subsonic general aviation and transport aircraft, with emphasis on layout, aerodynamic design, propulsion and performance, Springer Science & Business Media, 2013
- [18] Saarlas, M., Aircraft performance, John Wiley & Sons, 2006
- [19] Hepperle, M. Electric flight-potential and limitations, 2012
- [20] Traub, L. W., "Range and Endurance Estimates for Battery-Powered Aircraft," Journal of Aircraft, Vol. 48, No. 2, 2011, pp. 703–707.
- [21] Avanzini, G., and Giulietti, F., "Maximum Range for Battery-Powered Aircraft," Journal of Aircraft, Vol. 50, No. 1, 2013, pp. 304–307.
- [22] Patterson, M. D., German, B. J., and Moore, M. D., "Performance Analysis and Design of On-Demand Electric Aircraft Concepts," 12th AIAA Aviation Technology, Integration, and Operations Conference, AIAA Paper 2012-5474, Sept. 2012.
- [23] Sliwinski, J., Gardi, A., Marino, M., and Sabatini, R., "Hybrid-Electric Propulsion Integration in Unmanned Aircraft," Energy, Vol. 140, Dec. 2017, pp. 1407–1416.
- [24] Kuhn, H., Falter, C., and Sizmann, A., "Renewable Energy Perspectives for Aviation," Proceedings of the 3rd CEAS Air & Space Conference and 21st AIDAA Congress, Council of European Aerospace Societies, Brussels, Belgium, 2011, pp. 24–28.
- [25] Brelje, B. J., and Martins, J. R. R. A., "Electric, Hybrid, and Turboelectric Fixed-Wing Aircraft: A Review of Concepts, Models, and Design Approaches," Progress in Aerospace Sciences, Vol. 104, Jan. 2019, pp. 1–19.

MAXIMUM SPEED OF BATTERY-POWERED TILT-ROTOR

- [26] De Vries, R., Hoogreef, M. F., & Vos, R., "Range equation for hybrid-electric aircraft with constant power split," Journal of Aircraft, Vol. 57, No. 3, pp. 552-557, 2020
- [27] Bacchini, A., "Electric VTOL preliminary design and wind tunnel tests," Ph.D. Dissertation, Politecnico di Torino, 2020
- [28] Traub, L. W., "Range and endurance estimates for battery-powered aircraft." Journal of Aircraft, Vol. 48, No. 2, 2011, pp. 703-707.
- [29] Rossi, N. "Conceptual design of hybrid-electric aircraft," Master thesis, Politecnico di Milano, 2018.
- [30] Kadhiresan, A. R., & Duffy, M. J., "Conceptual design and mission analysis for eVTOL urban air mobility flight vehicle configurations," AIAA aviation 2019 forum, 2019, p. 2873.
- [31] Dommasch, D. O., Elements of Propeller and Helicopter Aerodynamics, Pitman Publishing Corporation, 1953. Chaps. 1-3.
- [32] Glauert, H., The Elements of Aerofoil and Airscrew Theory, 2nd Edition, Cambridge University Press, 1947.
- [33] Edwards, H. M., & Edwards, H. M. (1984). Galois theory, New York: Springer, 1984
- [34] Silva, C., Johnson, W., Antcliff, K.R. and Patterson, M.D., "VTOL urban air mobility concept vehicles for technology development," 2018 Aviation Technology, Integration, and Operations Conference, 2018, p.3847
- [35] Johnson, W., "A Quiet Helicopter for Air Taxi Operations," Proceedings of the 2020 VFS Aeromechanics for Advanced Vertical Flight Technical Meeting, San Jose, CA, Jan. 2020.
- [36] Whiteside, S.K.S., Pollard, B.P., Antcliff, K.R., Zawodny, N.S., Fei, X., Silva, C. and Medina, G.L, "Design of a Tiltwing Concept Vehicle for Urban Air Mobility," NASA TM-20210017971, 2021.

Copyright Statement

The authors confirm that they, and/or their company or organization, hold copyright on all of the original material included in this paper. The authors also confirm that they have obtained permission, from the copyright holder of any third party material included in this paper, to publish it as part of their paper. The authors confirm that they give permission, or have obtained permission from the copyright holder of this paper, for the publication and distribution of this paper as part of the ICAS proceedings or as individual off-prints from the proceedings.